

Heat capacities of alpha-iron(II) molybdate and iron(II) molybdate-II from 5 to 350 K^a

WILLIAM G. LYON^b and EDGAR F. WESTRUM, JR.^c

*Department of Chemistry, The University of Michigan,
Ann Arbor, Michigan 48104, U.S.A.*

(Received 16 December 1974; in revised form 3 February 1975)

Heat capacities of iron(II) molybdate-II (a metastable high-pressure phase) and of two samples of alpha-iron(II) molybdate were measured over the temperature range 5 to 350 K by means of adiabatic calorimetry. Rounding of lambda anomalies found at (43.0 ± 0.1) K for FeMoO₄-II and at (31.5 ± 0.1) K and (31.75 ± 0.1) K for two different samples of α -FeMoO₄ is attributed to impurity introduced by hitherto unreported slow air oxidation of these substances. Excess entropies associated with magnetic ordering were estimated as 1.11 cal_{th} K⁻¹ mol⁻¹ for FeMoO₄-II and 1.77 and 1.63 cal_{th} K⁻¹ mol⁻¹ for the two samples of α -FeMoO₄. At 298.15 K, the values of C_p° , S° , $\{H^\circ(T) - H^\circ(0)\}$, and $-\{G^\circ(T) - H^\circ(0)\}/T$, respectively, are 29.05 cal_{th} K⁻¹ mol⁻¹, 30.93 cal_{th} K⁻¹ mol⁻¹, 4852.3 cal_{th} mol⁻¹, and 14.656 cal_{th} K⁻¹ mol⁻¹ for FeMoO₄-II, and 28.31 cal_{th} K⁻¹ mol⁻¹, 32.7 cal_{th} K⁻¹ mol⁻¹, 4963 cal_{th} mol⁻¹, and 16.1 cal_{th} K⁻¹ mol⁻¹ (selected composite values) for α -FeMoO₄.

1. Introduction

The solid-state physical and chemical properties of the simple AMoO₄ molybdates have recently become important. Of current practical interest is their role in the oxidation of molybdenum alloys (*cf.* Brenner⁽¹⁾ and Rahmel *et al.*⁽²⁾), their possible use as host-lattices for paramagnetic ions (*cf.* Van Uitert *et al.*⁽³⁾), and their possible formation from high-yield fission products in nuclear fuel cells. Unlike the tungstates, the molybdates have few representatives as naturally occurring minerals; moreover, the most prominent of the naturally occurring molybdates, CaMoO₄ (powellite) and PbMoO₄ (wulfenite), are secondary minerals (*cf.* Palache *et al.*⁽⁴⁾). The fact that the primary mineral of molybdenum is the disulfide MoS₂, rather than a molybdate, has been convincingly rationalized by Urosov *et al.*⁽⁵⁾ on the basis of the thermochemical calculations for systems involving sulfides, tungstates, and molybdates. The considerable difference in geochemical behavior between tungsten

^a This work was supported in part by the Division of Research of the U.S. Atomic Energy Commission (AEC Cryogenics Project AT(11-1)-1149), and in recent months by the National Science Foundation (Project NSF GP-33424X).

^b Abstracted in part from a dissertation submitted in partial fulfillment of the requirements for the Ph.D. degree from the Horace H. Rackham School of Graduate Studies at The University of Michigan. Present address: Chemistry Division, Argonne National Laboratory, Argonne, Illinois 60439, U.S.A.

^c To whom correspondence concerning this paper should be directed.

and molybdenum indicates fundamental differences in the crystal chemistry and thermodynamics of tungstates and molybdates. To the understanding of this, accurate thermochemical and thermophysical studies can contribute.

The crystal chemistry of the AMoO_4 molybdates as a function of temperature and pressure has been recently reviewed by Sleight and Chamberland;⁽⁶⁾ the reader is referred to that review for a full discussion of their rather complex structures and their relationships to one another. The structure of $\alpha\text{-FeMoO}_4$ has been found by Sleight *et al.*⁽⁷⁾ to be of the $\alpha\text{-CoMoO}_4$ -type described by Smith and Ibers.⁽⁸⁾ Although the studies of Young and Schwartz⁽⁹⁾ and of Marshall⁽¹⁰⁾ were apparently consistent with the monoclinic symmetry expected for $\text{FeMoO}_4\text{-II}$ (high-pressure phase) having a structure of the NiWO_4 -type described by Keeling,⁽¹¹⁾ the subsequent single-crystal studies of Sleight *et al.*⁽⁷⁾ showed the structure to be a triclinic variant of the NiWO_4 -type.

The previous heat-capacity study of $\alpha\text{-FeMoO}_4$ from 50 to 300 K by Weller⁽¹²⁾ ignored the possibility of a magnetic transition below 50 K; hence, the thermal functions predicated upon a smooth extrapolation to $\tau = 0$ were likely to be significantly inaccurate. The magnetic-susceptibility studies of Sleight *et al.*⁽⁷⁾ (indicative of magnetic ordering in $\alpha\text{-FeMoO}_4$ and $\text{FeMoO}_4\text{-II}$ near 30 and 45 K, respectively) motivated low-temperature heat-capacity investigation of both materials over the 5 to 350 K range. These results permit a comparison of magnetic heat capacities not only between the two structures of iron(II) molybdate, but also between $\text{FeMoO}_4\text{-II}$ and the closely related FeWO_4 (*cf.* Lyon and Westrum⁽¹³⁾).

2. Experimental

SAMPLE CHARACTERIZATION

$\text{FeMoO}_4\text{-II}$

Dr A. W. Sleight prepared the sample of $\text{FeMoO}_4\text{-II}$ used in this research using hydrothermal methods described by Sleight *et al.*⁽⁷⁾ However, the synthesis was scaled up about thirty-fold to provide a sample of sufficient mass for the calorimetric measurements. Debye-Scherrer X-ray photographs ($\text{Cu K}\alpha$) made by Dr Sleight for the freshly prepared sample indicated no impurity lines from $\alpha\text{-Fe}_2\text{O}_3$, MoO_3 , or $\text{Fe}_2(\text{MoO}_4)_3$. Unfortunately, the ready oxidizability of this material was unanticipated, and the calorimetric sample was stored exposed to air for several months prior to the heat-capacity measurements.

Further X-ray work (Guinier, $\text{Cu K}\alpha$) was done after completion of the calorimetric measurements, because the rounded nature of the antiferromagnetic anomaly seemed an indication that the sample might have been contaminated. A complete tabulation of the measured d -spacings for this sample has been reported previously⁽¹⁴⁾ and is also available as a supplementary document.⁽¹⁵⁾ The triclinic lattice parameters obtained for this material in this research revealed no significant systematic deviations relative to the parameters determined by Sleight *et al.*⁽⁷⁾ indicative of distortions due to solid solution of impurities; a comparison of parameters is given in table 1.

Several distinct impurity lines were observed in the powder pattern for this

TABLE 1. Comparison of iron(II) molybdate-II lattice parameters for triclinic cell ^a

$\frac{a}{\text{nm}}$	$\frac{b}{\text{nm}}$	$\frac{c}{\text{nm}}$	α	β	γ	Reference
0.462	0.562	0.490	—	90° ^b	—	Young and Schwartz ⁽⁹⁾
0.469	0.569	0.494	—	90.25° ^b	—	Marshall ⁽¹⁰⁾
0.47078	0.57006	0.49443	90.67°	90.27°	87.68°	Sleight <i>et al.</i> ⁽⁷⁾
(4.708 ± 0.009) (5.703 ± 0.012) (4.936 ± 0.009) (90.62 ± 0.15) ^c (90.20 ± 0.22) ^c (87.73 ± 0.20) ^c This research ^c						

^a All parameters based on NiWO₄-type cell.

^b Cell thought to be monoclinic.

^c Guinier, Cu K α_1 using α -Si as an internal standard. Parameters are based on a least-squares fit of 33 indexed lines. Uncertainties are given as three standard deviations.

FeMoO₄-II sample. These have been determined to coincide with the strong lines corresponding to α -Fe₂O₃ (hematite). A sufficient number of such lines were present so that a set of lattice parameters (hexagonal) for the α -Fe₂O₃ impurity could be derived [$a = (0.5034 \pm 0.0009)$ nm; $c = (1.379 \pm 0.003)$ nm]. The parameters given in the Powder Diffraction File⁽¹⁶⁾ for a known pure α -Fe₂O₃ ($a = 0.50317$ nm; $c = 1.3737$ nm) differ only in the slightly smaller value for c ; whether this slight difference might be due to traces of molybdenum in the α -Fe₂O₃ impurity is a moot point. No impurity lines were found corresponding to MoO₃, α -FeMoO₄, or Fe₂(MoO₄)₃.

In contrast to the above, Dr Sleight⁽¹⁷⁾ has determined that initially clean samples of FeMoO₄-II stored at his laboratory for several years now show lines for α -Fe₂O₃, α -FeMoO₄, and Fe₂(MoO₄)₃ in the powder pattern (Guinier, Cr K α). The presence of traces of α -FeMoO₄ in aged samples of FeMoO₄-II provides confirmation of the conclusion of Sleight *et al.*⁽⁷⁾ that α -FeMoO₄ is the thermodynamically stable phase of ferrous molybdate at 298.15 K and 1 atm.†

Chemical analyses of the FeMoO₄-II sample for total iron and molybdenum are presented in table 2. Due to the mutual interference of iron and molybdenum in the analyses, and the necessity of an initial separation, the mole ratio $\{n(\text{Fe})/n(\text{Mo})\}$ is considered more reliably determined than the absolute percentages of Fe and Mo. Oxidative thermogravimetric analysis of FeMoO₄-II at this laboratory yielded a mass fraction of 0.7682 for FeMoO₄, corresponding to 25.67 mass per cent Fe (assuming an initial mole ratio $\{n(\text{Fe})/n(\text{Mo})\}$ of unity). Since this latter analysis was performed considerably later (January 1974) than the heat-capacity measurements, the value 0.7682 is taken as a lower bound on the phase purity of the calorimetric sample.

In addition to the solid-phase contaminants, the sample was determined (by calorimetric means) to contain 0.0202 mass per cent of H₂O. Further details of this determination are postponed until after the presentation of calorimetric results.

† Through this paper cal_{th} = 4.184 J; atm = 101.325 kPa; Torr = (101.325/760) kPa.

TABLE 2. Chemical analyses of iron(II) molybdates ^a, $w(\text{Fe})$ and $w(\text{Mo})$ are the mass fractions of Fe and Mo respectively, and $\{n(\text{Fe})/n(\text{Mo})\}$ is the mole ratio of Fe and Mo

Sample	$10^2w(\text{Fe})$	$10^2w(\text{Mo})$	$n(\text{Fe})/n(\text{Mo})$
FeMoO ₄ -II	25.79 ^b	43.71 ^d	1.014
	25.75 ^c	43.65 ^d	1.013
α -FeMoO ₄	25.03 ^b	42.87 ^d	1.003
(Dupont)	24.74 ^c	42.44 ^e	1.001
α -FeMoO ₄	25.02 ^b	42.72 ^d	
(Bureau of Mines)	24.60 ^c	42.62 ^d	0.999 ^{f, g}
FeMoO ₄ (Theory)	25.88	44.46	1.000
{2Fe ₂ O ₃ + 4MoO ₃ } (Theory)	24.96	42.87	1.000

^a Schwarzkopf Microanalytical Laboratory, Woodside, New York, February 1974.

^b Titration with K₂Cr₂O₇.

^c Specific colorimetry.

^d Precipitation as PbMoO₄ after extraction of Fe as phenanthroline complex.

^e Atomic absorption spectroscopy after extraction of Fe as phenanthroline complex.

^f This is an average value. Analyses for Fe and Mo were uncorrelated for this sample.

^g Weller's analytical results^(1,2) yielded 25.91 mass per cent Fe, 44.44 mass per cent Mo, and a mole ratio of 1.002.

α -FeMoO₄

Two samples of α -FeMoO₄ were used in this research. The first of these was the calorimetric sample used by Weller^(1,2) for his heat-capacity measurements in the 50 to 300 K range. In subsequent discussion, this sample will be denoted the "Bureau of Mines" sample. The second sample of α -FeMoO₄ (the "Dupont sample") was prepared by Dr A. W. Sleight according to methods described by Sleight *et al.*⁽⁷⁾ scaled up to produce a calorimetric sample of sufficient mass.

Debye-Scherrer photographs of the fresh samples showed no extra lines for oxides of iron or molybdenum for either sample. Since at the time the original X-ray work was done on the Bureau of Mines sample (*cf.* Weller^(1,2)) there were no data on pure α -FeMoO₄ available for comparison, it is possible that a contaminant such as Fe₂(MoO₄)₃ might have escaped detection in this sample. Both samples were stored exposed to air prior to the calorimetric measurements. For the Bureau of Mines sample, this exposure was many times greater; the sample had been evidently stored in contact with air ever since the measurements by Weller were completed.

Following the heat-capacity measurements of the present research, further X-ray powder patterns (Guinier, Cu K α) were made for both samples. As in the case of FeMoO₄-II, the roundedness of the transitions seemed an indication of possible sample contamination. The measured *d*-spacings were reported previously by Lyon⁽¹⁴⁾ and are also available in a supplementary document.⁽¹⁵⁾ These results give definite indications of contamination of both samples by α -Fe₂O₃, MoO₃, and Fe₂(MoO₄)₃. Two structures have been reported for Fe₂(MoO₄)₃. Nassau *et al.*⁽¹⁸⁾ and Trunov and Kovba⁽¹⁹⁾ have given parameters for an orthorhombic variety of this material; whereas, Plyasova *et al.*,⁽²⁰⁾ Klevtsov *et al.*,⁽²¹⁾ Marshall,⁽¹⁰⁾ and Sleight and Brixner⁽²²⁾ have investigated a monoclinic form. Kozmanov⁽²³⁾ and Jäger *et al.*⁽²⁴⁾ have reported powder patterns for Fe₂(MoO₄)₃ which neither agree

with each other nor may be convincingly indexed with the orthorhombic or monoclinic cell parameters. Sleight and Brixner⁽²²⁾ have concluded that the monoclinic phase is the stable phase at 298.15 K, but have found a sluggish diffusive transition near 772 K which may account for some of the discrepancies in the reported results. The present research indicates a separate phase (or phases) which correspond most closely with the pattern given by Kozmanov.⁽²³⁾ Additional impurity lines in α -FeMoO₄ were present which could not be indexed at all; however, many of these were probably weaker lines of the Fe₂(MoO₄)₃ phase(s) which were not observed or not reported by Kozmanov.⁽²³⁾

Dr Sleight⁽¹⁷⁾ has revealed that similar oxidation has occurred in initially uncontaminated samples of α -FeMoO₄ which had been stored for several years at his laboratory; X-ray powder patterns (Guinier, Cr K α) showed extra lines for α -Fe₂O₃ and Fe₂(MoO₄)₃. In contrast to the work on the calorimetric sample, however, no lines for MoO₃ were found.

Lattice parameters derived from the lines measured in this research for the two samples of α -FeMoO₄ are presented in table 3. In both cases, the lattice parameters

TABLE 3. Derived lattice parameters of α -ferrous molybdate ^a

Sample	<i>a</i> /nm	<i>b</i> /nm	<i>c</i> /nm	β
Sleight <i>et al.</i> ⁽⁷⁾	0.9805	0.8950	0.7660	114.05°
Dupont ^b	0.980 ± 0.001	0.895 ± 0.001	0.766 ± 0.001	(114.05 ± 0.09)°
Bureau of Mines ^c	0.979 ± 0.002	0.895 ± 0.002	0.765 ± 0.001	(114.0 ± 0.1)°

^a The uncertainties are three times the standard deviations from the least-squares fit of the measured lines.

^b Parameters based on least-squares fitting of 24 lines.

^c Parameters based on least-squares fitting of 28 lines.

are in close agreement with those determined by Sleight *et al.*⁽⁷⁾ Hence, despite suspicions concerning the purity of the predominant α -FeMoO₄ phase, firm evidence for contamination of this phase (*i.e.* evidence indicative of solid solution) was not obtained from the powder patterns. Nevertheless, the conclusion that the Dupont sample is the better sample can be supported by the fact that the powder pattern for this sample showed fewer impurity lines and had generally sharper lines for the α -FeMoO₄ phase.

Results of chemical analysis are presented in table 2 for both samples of α -FeMoO₄. No significant difference between samples is evident from these results, even though there is a considerable difference in color between the two; the Bureau of Mines sample had a slate-grey color, while the Dupont sample was black. As in the case of FeMoO₄-II, the mutual interference of Fe and Mo, render the absolute percentages of Fe and Mo somewhat suspect; the mole ratio is considered more reliably determined.

Oxidative thermogravimetric analysis of the α -FeMoO₄ samples conducted at this laboratory did not yield unambiguous results. Both samples, when heated in oxygen, undergo a mass loss (greater for the Bureau of Mines sample) just prior to

(and overlapping) mass gain from oxidation. The mass loss in both cases is believed due to the volatilization of free MoO_3 ; in the case of the Bureau of Mines sample, separate mass loss determinations in nitrogen indicate a loss of 0.48 per cent. However, the temperature at which mass loss occurs in N_2 is so much lower than in O_2 that it appears very dubious whether the identical process is occurring in each case. Indeed, calculations attempting to correct for mass loss as MoO_3 give results clearly at variance with the chemical analyses of table 2. From the t.g.a. results it was concluded not only that the samples of $\alpha\text{-FeMoO}_4$ are less pure than the sample of $\text{FeMoO}_4\text{-II}$, but also that the mass fraction of FeMoO_4 is in each case larger than 0.7.

HEAT CAPACITY MEASUREMENTS

Loading details and results. Heat capacity measurements for all three samples were made in the Mark II adiabatic cryostat.⁽²⁵⁾ Loading information for these samples is given in table 4. Heat capacities (or enthalpy increments) given in tables 5 through 7

TABLE 4. Calorimeter loading information: m is mass of sample and p the pressure of He added
(Torr = (101.325/760) kPa)

Compound	Mark-II Cryostat (A-5 Thermometer) ^a			
	Sample	Calorimeter ^b	m/g ^c	p/Torr ^d
$\alpha\text{-FeMoO}_4$	Dupont ^e	W-39 (23 cm ³)	34.7332	52
$\alpha\text{-FeMoO}_4$	Bureau of Mines ^f	W-42 (93 cm ³)	168.7785	86
$\text{FeMoO}_4\text{-II}$	Dupont ^g	W-39 (23 cm ³)	58.3746 (58.3630)	90

^a Westrum *et al.*⁽²⁵⁾.

^b Gold-plated copper calorimeters, laboratory designations.

^c Densities of 4.668 and 5.425 g cm⁻³ were used for the buoyancy corrections for $\alpha\text{-FeMoO}_4$ samples and for $\text{FeMoO}_4\text{-II}$, respectively. [Cf. Sleight *et al.*⁽⁷⁾]

^d Helium gas added to calorimeter to enhance thermal contact between sample and calorimeter-thermometer-heater assembly.

^e Sample loaded December 1968.

^f Sample loaded May 1969. Prior to loading, this sample was heated in vacuum to 600 K for 1 hr, during which time considerable outgassing occurred.

^g Sample loaded June 1969.

^h The sample mass less that of the separate phase H_2O is given in parentheses.

are expressed in terms of a molar mass of 215.7846 g mol⁻¹. Approximate temperature increments can usually be deduced from adjacent mean temperatures. Molar heat-capacity curves for $\text{FeMoO}_4\text{-II}$ and $\alpha\text{-FeMoO}_4$ are displayed in figures 1 and 2, respectively.

Heat capacity of $\text{FeMoO}_4\text{-II}$. The major feature of the heat capacity of $\text{FeMoO}_4\text{-II}$ is a rounded bump whose maximum in the *total* heat capacity is located at (43.0 ± 0.1) K. Since the anomaly is a rounded one, the temperature of the maximum in the magnetic (excess) heat capacity need not be identical, but may vary somewhat, depending on the choice of lattice heat capacity.

TABLE 5. Experimental heat capacity of iron(II) molybdate-II ^a
(cal_{th} = 4.184 J)

T K	C_p cal _{th} K ⁻¹ mol ⁻¹	T K	C_p cal _{th} K ⁻¹ mol ⁻¹	T K	C_p cal _{th} K ⁻¹ mol ⁻¹	T K	C_p cal _{th} K ⁻¹ mol ⁻¹
Series I							
158.76	18.85	52.27	5.691	124.28	14.71	9.81	0.162
164.46	19.40	56.73	5.651	132.19	15.70	10.92	0.208
170.01	20.01	63.12	6.201	140.40	16.72	12.21	0.253
Series II							
178.37	20.84	71.36	7.206	Series IX			
184.51	21.52	80.05	8.460	136.03	16.17	14.91	0.433
190.89	21.98	87.00	9.515	144.18	17.14	16.23	0.532
197.32	22.53	92.77	10.34	156.49	18.56	17.78	0.665
203.70	23.03	Series VI		164.66	19.43	19.59	0.849
Series III							
216.43	23.96	96.73	10.91	172.79	20.27	21.52	1.078
222.81	24.65	102.22	11.67	180.83	21.04	23.82	1.397
229.27	25.07	107.73	12.50	188.74	21.75	26.46	1.826
235.71	25.38	113.15	13.21	Series X			
242.14	26.05	118.62	13.94	191.56	21.97	29.11	2.337
248.57	26.30	124.16	14.65	201.28	22.82	31.89	2.978
254.99	26.79	129.68	15.39	211.06	23.63	34.72	3.812 ^b
261.42	27.11	135.26	16.08	221.00	24.40	37.22	4.761 ^b
267.81	27.56	140.96	16.73	231.09	25.18	40.06	6.101 ^b
274.13 ^a		Series VII		241.36	25.86	44.28	6.729 ^b
280.42	28.33	62.54	6.148	251.82	26.49	Series XII ^a	
Series IV							
292.71	28.97	68.41	6.817	262.46	27.17	43.65	6.795
298.98	29.36	73.98	7.566	273.20 ^a	28.39	47.54	6.242
305.27	29.68	79.42	8.355	284.02	28.92	51.54	5.702
311.51	29.78	84.66	9.162	294.96	29.92	55.56	5.600
317.76	30.03	89.75	9.893	305.98	29.49	59.44	5.738
324.03	29.92	Series VIII		324.08	30.17	63.59	6.243
330.24	30.67	78.53	8.224	335.22	30.64	68.17	6.780
336.49	30.16	83.59	8.999	343.94	30.97	Series XIII ^b	
343.60	30.98	89.00	9.812	349.67	31.16	33.11	3.323
Series V							
Series VI							
Series VII							
Series VIII							
Series IX							
Series X							
Series XI							
Series XII ^a							
Series XIII ^b							

^a Water fusion anomaly.^b No correction for curvature.

In addition to the rounded magnetic anomaly, the heat capacity of FeMoO₄-II revealed a small bump located close to 273 K, which is believed to result from the fusion of water. The hydrothermal origin of this sample and the lack of such a bump in samples of α-FeMoO₄ tends to support this interpretation more than any other (e.g. magnetic impurities, etc.). From the excess enthalpy in the region of this small bump, a value of 0.0202 mass per cent of H₂O was computed by making use

TABLE 6. Enthalpy determinations of iron(II) molybdates
(cal_{th} = 4.184 J)

Designation	$\frac{T_1}{K}$	$\frac{T_2}{K}$	$\frac{H(T_2) - H(T_1)}{\text{cal}_{th} \text{ mol}^{-1}}$	$\frac{H(60 K) - H(30 K)}{\text{cal}_{th} \text{ mol}^{-1}}$
FeMoO ₄ -II				
A (Series XIV)	29.86	59.93	162.078	162.147
B (Series XV)	30.40	60.10	161.588	162.048
Series XIII	31.53	53.98	123.717	161.965
				Average: 162.053 ± 0.06
α-FeMoO ₄ (Bureau of Mines Sample)				
A (Series VI)	25.23	38.03	48.623	55.803
B (Series VI)	28.23	39.42	43.605	55.848
C (Series VIII)	24.27	39.10	55.405	55.711
Series V	24.27	35.38	41.309	55.763
				Average: 55.781 ± 0.06

TABLE 7. Experimental heat capacities of alpha-iron(II) molybdates
(cal_{th} = 4.184 J)

$\frac{T}{K}$	$\frac{C_p}{\text{cal}_{th} \text{ K}^{-1} \text{ mol}^{-1}}$	$\frac{T}{K}$	$\frac{C_p}{\text{cal}_{th} \text{ K}^{-1} \text{ mol}^{-1}}$	$\frac{T}{K}$	$\frac{C_p}{\text{cal}_{th} \text{ K}^{-1} \text{ mol}^{-1}}$	$\frac{T}{K}$	$\frac{C_p}{\text{cal}_{th} \text{ K}^{-1} \text{ mol}^{-1}}$
Dupont Sample							
Series I		156.19	19.41	339.78	30.04	12.44	0.659
250.77	26.27	163.86	20.14	347.03	30.35	15.67	0.869
259.61	26.71	172.04	20.85			18.76	1.351
268.33	27.12	180.76	21.58			21.21	1.850
276.93	27.56	189.34	22.24	Series IV ^a		23.41	2.394
286.05	27.96	198.69	22.94	5.79	0.061	25.61	3.106
296.06	28.44	205.84	23.48	6.26	0.097	28.24	4.118
307.60	28.92	214.40	24.04	7.76	0.189	32.13	4.366
319.91	29.42	223.38	24.62	8.44	0.285	37.02	3.971
332.05	29.88	232.38	25.16	8.95	0.226	41.53	4.355
		241.40	25.69	9.64	0.300	45.99	4.910
				10.15	0.309	51.16	5.631
Series II				10.82	0.437		
69.24	8.356			11.60	0.646		
73.45	8.963	Series III		12.87	0.686		
79.38	9.887	248.46	26.10	14.94	0.780	Series VI	
86.39	10.97	257.68	26.62	16.99	1.062	56.75	6.439
94.25	12.09	266.99	27.11	18.87	1.374	62.54	7.325
102.12	13.15	276.34	27.57	20.86	1.773	68.43	8.214
109.41	14.12	285.79	27.99			74.77	9.166
116.93	15.08	295.39	28.41			82.28	10.38
124.75	16.04	314.91	29.19	Series V ^a		90.90	11.50
132.20	16.91	324.36	29.50	6.44	0.095	98.23	12.62
148.26	18.64	332.51	29.93	9.44	0.293	107.48	13.86

TABLE 7—(continued)

T K	C_p cal _{th} K ⁻¹ mol ⁻¹	T K	C_p cal _{th} K ⁻¹ mol ⁻¹	T K	C_p cal _{th} K ⁻¹ mol ⁻¹	T K	C_p cal _{th} K ⁻¹ mol ⁻¹
Bureau of Mines Sample							
Series I		Series IV		30.05	3.985	32.65	4.041
62.22	7.170	259.92	26.70	30.62	4.073	32.98	3.955
69.79	8.315	270.76	27.22	31.05	4.118	33.35	3.862
76.88	9.393	281.31	27.74	31.37	4.166	33.81	3.772
84.16	10.53	291.70	28.23	31.69	4.169	34.72	3.704
91.92	11.67	301.89	28.62			12.80	0.640
99.72	12.74	311.98	29.11			14.54	0.737
		321.93	29.41	Series VI ^a		16.67	1.008
		331.76	29.80	7.23	0.089	18.68	1.342
		339.50	30.12	8.67	0.152	22.15	2.078
Series II		345.29	30.20	9.36	0.199	25.55	3.105
109.63	14.27			10.41	0.276	27.37	3.726
117.37	15.09			11.35	0.609	Enthalpy Det'n. B	
125.70	16.09			12.25	0.633		
134.51	17.11	Series V ^a		13.29	0.654		
143.71	18.11	11.02	0.337	14.31	0.691	Series VIII	
153.14	19.06	11.38	0.393	15.52	0.842	Enthalpy Det'n. C	
162.89	19.95	11.91	0.640	16.98	1.053	40.03	4.075
172.99	20.88	13.02	0.614	18.50	1.301	42.44	4.355
183.23	21.72	14.54	0.748	20.31	1.650	45.42	4.736
193.65	22.54	16.34	0.968	22.33	2.099	48.44	5.149
		18.34	1.287	24.28	2.641	51.43	5.565
		20.23	1.646	Enthalpy Det'n. A		54.39	5.991
		21.92	1.998	40.30	4.110 ^b	57.35	6.429
Series III		23.50	2.397			60.30	6.877
204.13	23.31	25.05	2.898	Series VII		63.79	7.413
215.02	24.07	26.52	3.495			67.80	8.024
226.26	24.76	27.86	3.797	32.01	4.165	71.85	8.630
237.62	25.46	29.13	3.864	32.33	4.104	75.93	9.248
248.94	26.11						

^a These series were not curvature corrected.⁽¹⁵⁾

^b Curvature corrected.

of the value, 143.63 cal_{th} mol⁻¹, for the enthalpy of fusion of pure water given in Circular 500.⁽²⁶⁾

Heat capacity of α-FeMoO₄. The heat capacities of the two samples of α-FeMoO₄ show rounded bumps located at (30.5±0.1) and (31.75±0.1) K (in the total heat capacities) for the Dupont and Bureau of Mines samples, respectively. The anomaly for the Bureau of Mines sample showed a slight shoulder at temperatures just below the peak minimum. In the region of the rounded anomaly and at higher temperatures, the Dupont sample has a slightly higher heat capacity than the Bureau of Mines sample. Below 20 K, the heat capacities of both samples are nearly identical. At temperatures between 12 and 13 K both samples exhibited a small additional bump for which it was found difficult to make consistent sets of measurements. The small size of the anomaly and the uncertainty in the results in this region, made it difficult to determine the shape of this anomaly; however, it appears to be a very small finite peak rather than a sharp discontinuity.

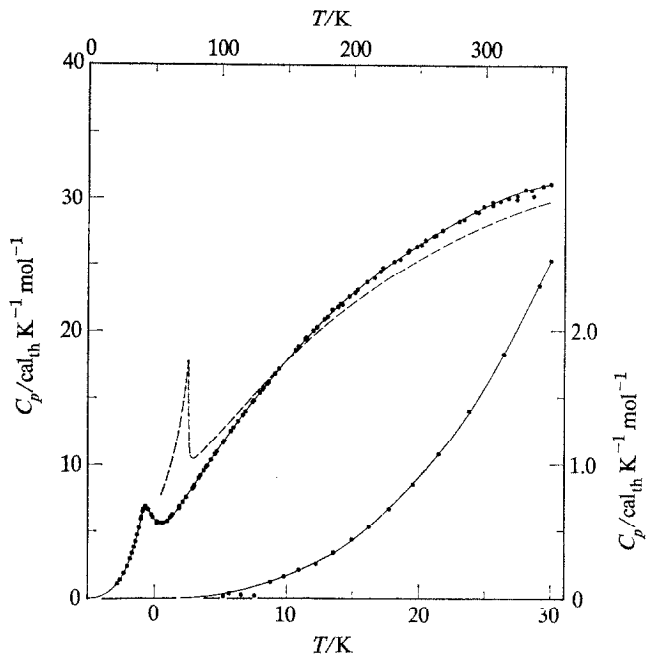


FIGURE 1. Heat capacity of $\text{FeMoO}_4\text{-II}$. ●, this work; ---, reference 13.

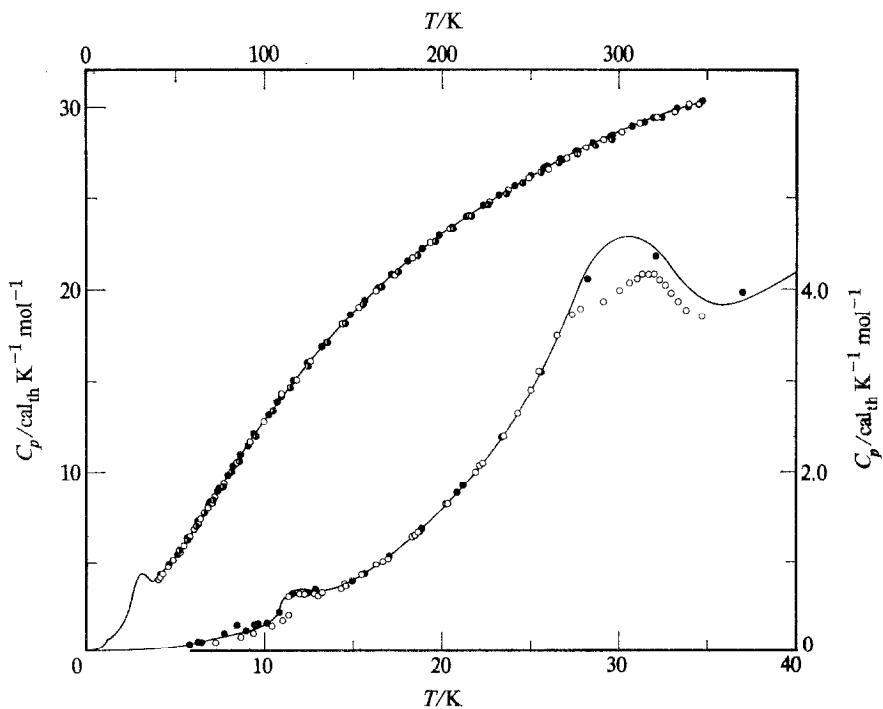


FIGURE 2. Heat capacity of $\alpha\text{-FeMoO}_4$. ●, this work, Dupont sample; ○, this work, Bureau of Mines sample; ●, Weller;⁽¹²⁾ —, results for Dupont sample.

CALCULATIONS

Impurity corrections. Adjustment for the small amount of the water in the sample of $\text{FeMoO}_4\text{-II}$ was made on the experimental heat capacity by the use of the heat capacity of pure water determined by Giauque and Stout.⁽²⁷⁾ These corrections have been made on all results given in table 5, with the exception of the two points at the peak of the water fusion bump. These latter points have only their temperature listed.

No corrections were attempted for the separate oxidation products present in the samples of ferrous molybdate. The data in table 5 through 7 are, therefore, the *apparent* molar heat capacities of the three samples, calculated as if they were free of oxidation products.

Thermal functions. The experimental heat capacities for the non-transition regions were curve-fitted to polynomials in reduced temperature by the method of least-squares and then integrated to yield values of the thermal functions at regular temperature intervals. The thermal functions in the transition regions are based on enthalpy determinations covering the transition maxima and on numerical integration of heat capacities read from large scale plots of the transition regions. At temperatures below the low temperature limit of the measurements, entropy and enthalpy increments were obtained from plots of C_p/T against T^2 . No attempt was made in the process of extrapolation to adjust for contributions due to isotopic mixing or nuclear spin; hence, the values tabulated are practical values of the thermal functions for use in ordinary thermochemical calculations.

TABLE 8. Thermal functions of iron(II) molybdate-II
($\text{cal}_{\text{th}} = 4.184 \text{ J}$)

T K	C_p $\text{cal}_{\text{th}} \text{K}^{-1} \text{mol}^{-1}$	$\{S^\circ(T) - S^\circ(0)\}$ $\text{cal}_{\text{th}} \text{K}^{-1} \text{mol}^{-1}$	$\{H^\circ(T) - H^\circ(0)\}$ $\text{cal}_{\text{th}} \text{K}^{-1} \text{mol}^{-1}$	$-\{G^\circ(T) - H^\circ(0)\}/T$ $\text{cal}_{\text{th}} \text{K}^{-1} \text{mol}^{-1}$
25	1.578	0.622	11.194	0.174
50	5.862	3.579	126.66	1.026
75	7.719	6.109	284.43	2.317
100	11.385	8.834	523.4	3.600
150	17.83	14.712	1259.2	6.318
200	22.73	20.55	2280.3	9.152
250	26.41	26.03	3511.9	11.987
298.15	29.05	30.93	4852.3	14.656
300	29.13	31.11	4906.1	14.757
350	31.19	35.76	6415	17.43

Values of the thermal functions for $\text{FeMoO}_4\text{-II}$ are presented in an abbreviated form in table 8 and in the usual manner in the supplementary document.⁽¹⁵⁾ Selection of a suitable composite set of thermal functions for $\alpha\text{-FeMoO}_4$ has proven problematical; however, table 9 compares heat capacity, enthalpy, and entropy increments from this research and that of Weller.⁽¹²⁾

TABLE 9. Comparison of the thermal functions of α -ferrous molybdate samples ($\text{cal}_{\text{th}} = 4.184 \text{ J}$)

	Dupont	Bureau of Mines	Weller ^a
T/K		$C_p/\text{cal}_{\text{th}} \text{K}^{-1} \text{mol}^{-1}$	
50	5.47	5.37	5.31
75	9.22	9.12	9.11
100	12.89	12.80	12.71
150	18.78	18.74	18.67
200	23.06	23.00	22.93
250	26.25	26.17	26.08
298.15	28.52	28.48	28.31
300	28.60	28.56	—
350	30.43	30.40	—
$\{H^\circ(50 \text{ K}) - H^\circ(0)\}/\text{cal}_{\text{th}} \text{mol}^{-1}$	128.66	124.20	(84.28) ^b
$\{H^\circ(298.15 \text{ K}) - H^\circ(50 \text{ K})\}/\text{cal}_{\text{th}} \text{mol}^{-1}$	4870	4853	4834
$\{H^\circ(298.15 \text{ K}) - H^\circ(0)\}/\text{cal}_{\text{th}} \text{mol}^{-1}$	4998	4977	(4918)
$S^\circ(50 \text{ K})/\text{cal}_{\text{th}} \text{K}^{-1} \text{mol}^{-1}$	4.08	3.94	(2.31) ^b
$\{S^\circ(298.15 \text{ K}) - S^\circ(50 \text{ K})\}/\text{cal}_{\text{th}} \text{K}^{-1} \text{mol}^{-1}$	28.84	28.70	28.60
$S^\circ(298.15 \text{ K})/\text{cal}_{\text{th}} \text{K}^{-1} \text{mol}^{-1}$	32.92	32.64	(30.91)
Provisional thermal functions at $T = 298.15 \text{ K}^\circ$			
$C_p^\circ/\text{cal}_{\text{th}} \text{K}^{-1} \text{mol}^{-1} = 28.31$		$\{H^\circ(T) - H^\circ(0)\}/\text{cal}_{\text{th}} \text{mol}^{-1} = 4963$	
$S^\circ/\text{cal}_{\text{th}} \text{K}^{-1} \text{mol}^{-1} = (32.7 \pm 0.1)$		$-\{G^\circ(T) - H^\circ(0)\}T^{-1}/\text{cal}_{\text{th}} \text{K}^{-1} \text{mol}^{-1} = 16.1$	

^a Reanalyzed Weller⁽¹²⁾ results on Bureau of Mines sample.

^b The parenthetic values represent smooth extrapolations made on the basis of the representation of the heat capacity in the 50 to 298.15 K range as a combination of Debye and Einstein functions given by Weller.⁽¹²⁾ Such an extrapolation obviously neglects the possibility of a transition below 50 K.

^c The selected values are a combination of the results from the Dupont sample below 50 K, and of the results from Weller's sample from 50 to 298.15 K.

The thermal functions for all three samples of iron(II) molybdate are considered to have a precision corresponding to a probable error of less than 0.1 per cent above 100 K.

3. Discussion

MAGNETIC CONTRIBUTIONS TO THE HEAT CAPACITY

FeMoO₄-II

The temperature, $(43.0 \pm 0.1) \text{ K}$, of the peak maximum in the (total) heat capacity correlates well with the temperature, $(45 \pm 5) \text{ K}$, of the maximum in magnetic susceptibility determined by Sleight *et al.*⁽⁷⁾ However, the rounded character of the observed anomaly is different from the usual sharp "lambda" shape ordinarily associated with the onset of magnetic ordering (*cf.* Stout⁽²⁸⁾).

Some insight into the problem of analyzing the magnetic contribution to the heat capacity for FeMoO₄-II may be obtained from an examination of figure 1 which

contrasts the heat capacities of $\text{FeMoO}_4\text{-II}$ and FeWO_4 . In view of the fact that these two materials are roughly iso-structural, the differences are quite remarkable. Most notable is the fact that the heat capacity of $\text{FeMoO}_4\text{-II}$ greatly exceeds that of FeWO_4 in the region above 200 K, despite the fact that the molar mass of the latter compound is considerably greater (by a factor of about 1.4) than that of the former. While it is not necessarily unusual for the heat capacities of molybdenum compounds to exceed those of the analogous tungsten compounds (*cf.* King *et al.*⁽²⁹⁾) for a comparison of the compounds, MoO_3 , WO_3 , MoO_2 , and WO_2) such an effect practically annihilates any hope of analyzing the lattice heat capacity of $\text{FeMoO}_4\text{-II}$ through adjustment of the heat capacity of an iso-structural tungstate. Large differences in heat capacity could arise from a combination of differences in lattice dynamics and in electronic contributions to the heat capacity; the analysis of the relative importance of these two possibilities would require heat capacities for $\text{ZnMoO}_4\text{-II}$.

The transition region of $\text{FeMoO}_4\text{-II}$ is depicted in detail in figure 3 with a splined interpolation of the lattice heat capacity. The lattice estimate selected here is a

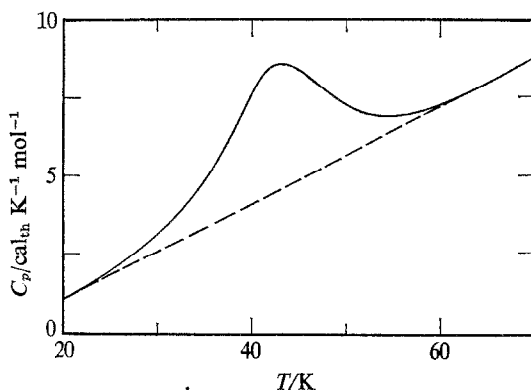


FIGURE 3. Heat capacity of $\text{FeMoO}_4\text{-II}$ in the transition region. —, experimental; ---, estimated lattice heat capacity.

maximal one; *i.e.* the chosen curve is a smooth extrapolation under the obviously anomalous region, and thus may tend to under-estimate the magnetic heat capacities in both the spin-wave and the short-range ordering regions. Based on this lattice, the excess enthalpy and entropy associated with the anomaly are $46.2 \text{ cal}_{\text{th}} \text{ mol}^{-1}$ and $1.11 \text{ cal}_{\text{th}} \text{ K}^{-1} \text{ mol}^{-1}$, respectively.

Such a value for the excess entropy is rather surprising. Transitions with excess entropies near $R \ln 2$ have been observed previously for iron(II) compounds [*e.g.* FeCl_2 ⁽²⁸⁾ and FeCO_3 ⁽³⁰⁾]; however, in these instances the site symmetry of the Fe^{2+} ions is higher (D_{3d}), and the entropies appear to be a reasonable consequence of the pattern of crystal field splitting (*cf.* Kanamori⁽³¹⁾). In $\text{FeMoO}_4\text{-II}$, the triclinic symmetry of the crystal would suggest that the pattern of energy levels should be similar to FeWO_4 . Indeed, the quadruple splittings derived by Sleight *et al.*⁽⁷⁾ from Mössbauer spectra at 4.2, 78, and 297 K show so little temperature variation that

low-lying electronic energy levels seem ruled out.⁽³²⁾ Nevertheless, the possibility remains that a ground-state doublet separated by many hundreds of cm^{-1} from the excited states exists here.

An alternate possibility is that sample impurities and/or poor choice of lattice heat capacity has misled these authors to a value of the excess entropy, only one-third of $R \ln 5$. The anomaly depicted in figure 3 is remarkable for the high degree of symmetry exhibited near the peak of the transition. The nearly Gaussian shape of the excess heat capacity occasions some concern over the true extent of the anomaly on the high-temperature side. Since the *total* entropy of $\text{FeMoO}_4\text{-II}$ at 50 K barely exceeds $R \ln 5$, the region of short-range ordering in $\text{FeMoO}_4\text{-II}$ would have to be remarkably large to achieve the excess entropy of $R \ln 5$ that might be expected from magnetic ordering analogous to that in FeWO_4 . Although a more secure basis for estimating the lattice heat capacity would be required to rule out the latter possibility with assurance, an excess entropy as large as $R \ln 5$ would be possible if the impurities have a disproportionately large effect on the transition.

$\alpha\text{-FeMoO}_4$

The transition regions for both samples of $\alpha\text{-FeMoO}_4$ are depicted in figure 4. The temperatures of the peak maxima for the large anomalies, (30.5 ± 0.1) and (31.75 ± 0.1) K, for the Dupont and Bureau of Mines samples, respectively, correlate

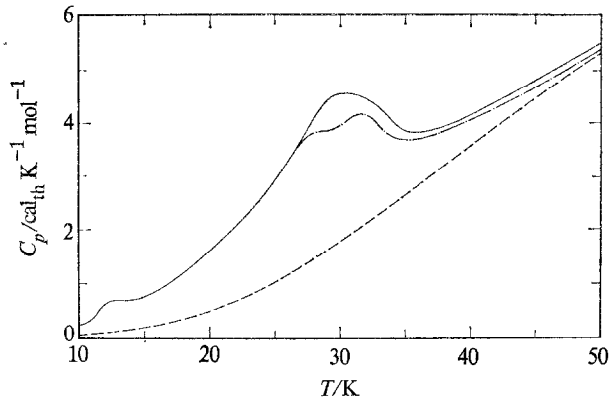


FIGURE 4. Heat capacity of $\alpha\text{-FeMoO}_4$ in the transition region. —, experimental, Dupont sample; — · —, experimental, Bureau of Mines sample; ---, estimated.

well with the maximum, at a temperature of (30 ± 5) K, in magnetic susceptibility observed by Sleight *et al.*⁽⁷⁾ but not identified as the onset of magnetic ordering. Whatever the origin of the peculiar magnetic behavior, it is clear from the present heat capacities that $\alpha\text{-FeMoO}_4$ shows very complex behavior below 50 K, and that (at least) two bumps appear in the heat capacity. The small anomalies, appearing at 12 to 13 K in the heat capacities of both samples, are either non-magnetic in origin, or else of sufficiently small size so that the effect escaped detection in the magnetic-susceptibility measurements.

Estimating the lattice heat capacity throughout the anomalous region is here further complicated by the overlapping of two transition regions. No attempt will be made in this analysis to resolve separately the excess entropies of these two transitions.

Use of Weller's⁽¹²⁾ smooth extrapolation of the heat capacity of α -FeMoO₄ (in Debye and Einstein functions) as a lattice heat capacity, results in values of the excess entropy of 1.77 and 1.63 cal_{th} K⁻¹ mol⁻¹ associated with the entire anomalous regions of the Dupont and Bureau of Mines samples, respectively. In these cases also, the relatively low values of the excess entropy seem rather surprising in view of the low site symmetry of the Fe²⁺ ions.

The crystal structure of α -FeMoO₄ permits two different kinds of sites for the Fe²⁺ ions (mirror planes or diagonal axes); however, the environments of the two kinds of Fe²⁺ ions must be very similar, since the room temperature Mössbauer spectrum of Sleight *et al.*⁽⁷⁾ failed to distinguish them. At a temperature of 4.2 K, the Mössbauer spectrum—while not showing a clear-cut magnetic hyperfine pattern—does show quadruple-split absorption peaks consistent with two different iron sites. The strong variation of the quadruple splittings computed by these authors from the spectra at 4.2, 78, 246, and 297 K seems strongly indicative of very low-lying energy levels (*cf.* Ingalls⁽³²⁾).

The present heat-capacity results, which clearly indicate an extensive cooperative anomaly at temperatures below 50 K, tend to support the contention that some kind of magnetic ordering is taking place. Possibly the small transition at 12 to 13 K is associated with a volume distortion or alteration of magnetic structure sufficient to render the two types of Fe²⁺ ions distinguishable in the Mössbauer spectrum at 4.2 K. To be completely consistent with the Mössbauer results at 4.2 K, the process of magnetic ordering would have to result, according to Sleight *et al.*⁽⁷⁾ in effective internal magnetic fields about ten times smaller than usually observed for iron(II) compounds. A more detailed examination of Mössbauer spectra as a function of temperature throughout the anomalous region should prove useful in resolving this apparent conflict. If, indeed, the effective internal fields are of so small a magnitude, it may be possible to induce ferromagnetism in this material by applying relatively small external magnetic fields; such experiments would provide a further test of the explanation favored by us.

EFFECTS OF IMPURITIES

In non-transition regions, various calculations of the effects of the impurities present as separate phases in these FeMoO₄ samples indicate that apparent heat capacities would be only slightly increased over true heat capacities⁽¹⁵⁾ (up to 0.7 per cent). These calculations are in good accord with the measured heat-capacity spread of α -FeMoO₄.

In the transition region, however, the direct effect of separate phase impurities is more serious. On the assumption that the mass fraction of FeMoO₄ at the time of the heat capacity measurement was 0.77 or greater, the excess entropy of the magnetic anomaly in the FeMoO₄-II sample may be adjusted to a value of 1.44 cal_{th} K⁻¹ mol⁻¹; hence, it is unlikely that separate phase impurities alone would account for an apparent

excess entropy so much less than $R \ln 5$ ($3.20 \text{ cal}_{\text{th}} \text{ K}^{-1} \text{ mol}^{-1}$). The assumption of similar levels of separate phase contaminants for the samples of $\alpha\text{-FeMoO}_4$ at the time of heat capacity measurement would yield adjusted values of $2.30 \text{ cal}_{\text{th}} \text{ K}^{-1} \text{ mol}^{-1}$ and $2.12 \text{ cal}_{\text{th}} \text{ K}^{-1} \text{ mol}^{-1}$, respectively, for the excess entropies of the Dupont and Bureau of Mines samples. Here too, it is unlikely that separate phase impurities alone could account for an apparent excess entropy so much less than $R \ln 5$; however, an entropy greater than $R \ln 2$ seems indicated.

The rounding of heat-capacity peaks because of hidden variables is not a well understood subject either theoretically⁽³³⁾ or empirically.⁽¹⁵⁾ Within the precision of the X-ray characterization, no deviations of lattice parameters indicative of solid solution (e.g. of Fe^{3+} ions) were noted. Hence, the probable cause of rounding in these samples is not supported by direct evidence. Because of the possibility of a disproportionate effect for this type of impurity on the excess entropy, the present conclusions are somewhat guarded.

We thank Dr E. G. King of the Albany Metallurgy Research Center, U.S. Bureau of Mines, Albany, Oregon for the loan of a sample of $\alpha\text{-FeMoO}_4$, and Dr A. W. Sleight of the Central Research Department of E. I. du Pont de Nemours and Company, Wilmington, Delaware, for samples of $\alpha\text{-FeMoO}_4$ and $\text{FeMoO}_4\text{-II}$. P. F. Finamore and K. Gerst assisted with many of the experimental measurements and calculations. Assistant Professor J. Haschke of the Department of Chemistry, The University of Michigan, gave much valuable advice and assistance with the X-ray measurements and calculations.

REFERENCES

1. Brenner, S. S. *J. Electrochem. Soc.* **1955**, 102, 7.
2. Rahmel, A.; Jäger, W.; Becker, K. *Arch. Eisenhüttenw.* **1959**, 30, 351.
3. Van Uitert, L. G.; Swanekamp, F. W.; Preziosi, S. J. *Appl. Phys.* **1961**, 32, 1176.
4. Palache, C.; Berman, H.; Frondel, C. *Dana's System of Mineralogy*, Vol. II. Seventh Edition. John Wiley and Sons, Inc.: New York. **1951**, pp. 1079-86.
5. Urosov, V. S.; Ivanova, G. F.; Khodakovskii, I. L. *Geokhimiya* **1967**, 1050.
6. Sleight, A. W.; Chamberland, B. L. *Inorg. Chem.* **1968**, 7, 1672.
7. Sleight, A. W.; Chamberland, B. L.; Weiher, J. F. *Inorg. Chem.* **1968**, 7, 1093.
8. Smith, G. W.; Ibers, J. S. *Acta Cryst.* **1965**, 19, 269.
9. Young, A. P.; Schwartz, C. M. *Science* **1963**, 141, 348.
10. Marshall, D. J. *J. Mater. Sci.* **1967**, 2, 294.
11. Keeling, R. O. *Acta Cryst.* **1957**, 10, 209.
12. Weller, W. W. *U.S. Bur. Mines, Rep. Invest.* 6782, **1966**.
13. Lyon, W. G.; Westrum, E. F., Jr. *J. Chem. Thermodynamics* **1974**, 6, 763.
14. Lyon, W. G., Ph.D. Thesis, The University of Michigan, Ann Arbor, Michigan, **1973**. *Diss. Abst.*, **1975**, 35, Issue 1, 75-15790.
15. Detailed supplementary data concerning X-ray and chemical analyses of the samples used in this research, see NAPS document No. 02553 for 29 pages of supplementary material. Order from ASIS/NAPS, c/o Microfiche Publications, 305 E. 46th St., New York, N.Y. 10017. Remit in advance for each NAPS accession number. Make checks payable to Microfiche Publications. Photocopies are \$5.00. Microfiche are \$1.50. Outside of the U.S. or Canada, postage is \$2.00 for a PC or \$0.50 for a fiche.
16. Joint Committee on Powder Diffraction Standards, Inc., 1601 Park Lane, Swarthmore, PA. Card #13-0534.
17. Sleight, A. W.; personal communication.
18. Nassau, K.; Levinstein, H. J.; Loicono, G. M. *J. Phys. Chem. Solids* **1965**, 26, 1805.

19. Trunov, V. K.; Kovba, L. M. *Izv. Akad. Nauk SSSR, Neorgan. Mater.* **1966**, 2, 151.
20. Plyasova, L. M.; Klevtsova, R. F.; Borisov, S. V.; Kefeli, L. M. *Dokl. Akad. Nauk SSSR* **1965**, 167, 84. (Cf. *Soviet Physics—Doklady* **1966**, 11, 189.)
21. Klevtsov, P. V.; Kefeli, L. M.; Plyasova, L. M. *Izv. Akad. Nauk SSSR, Neorgan. Mater.* **1965**, 1, 918.
22. Sleight, A. W.; Brixner, L. H. *J. Solid State Chem.* **1973**, 7, 172.
23. Kozmanov, Yu. D. *Zh. Fiz. Khim.* **1957**, 31, 1861.
24. Jäger, W.; Rahmel, A.; Becker, K. *Arch. Eisenhüttenw.* **1959**, 30, 435.
25. Westrum, E. F., Jr.; Furukawa, G. T.; McCullough, J. P. Adiabatic low-temperature calorimetry. Chap. 5 in *Experimental Thermodynamics*, Vol. I. McCullough, J. P.; Scott, D. W.; editors. Butterworths: London. **1968**, p. 133.
26. Rossini, F. D.; Wagman, D. D.; Evans, W. H.; Levine, S.; Jaffe, I. *National Bureau of Standards Circular No. 500*. U.S. Government Printing Office, Washington, D.C. **1952**.
27. Giauque, W. F.; Stout, J. W. *J. Amer. Chem. Soc.* **1939**, 58, 1144.
28. Stout, J. W. *Pure Appl. Chem.* **1961**, 2, 287.
29. King, E. G.; Weller, W. W.; Christensen, A.U. *U.S. Bur. Mines Rep. Invest. 5664*, **1960**.
30. Kalinkina, I. N. *Zh. Eksperim. i Teor. Fiz.* **1962**, 43, 2028. (Cf. *Soviet Physics—JETP* **1963**, 16, 1432.)
31. Kanamori, J. *Progr. Theoret. Phys.* (Japan) **1958**, 20, 890.
32. Ingalls, R. *Phys. Rev.* **1964**, 133, A787.
33. Fisher, M. E. *Phys. Rev.* **1968**, 176, 257.